Correlations between the production of hydroxyl radical/hydrogen and the maximum temperature and pressure reached inside acoustic bubbles

KERABCHI Nassim [A]*, MEROUANI Slimane [A,b], HAMDAOUI Oualid [A]

[a] Laboratory of Environmental Engineering, Department of Process Engineering, Faculty of Engineering, Badji Mokhtar – Annaba University, P.O. Box 12, 23000 Annaba, Algeria

[b] Laboratory of Environmental Process Engineering, Faculty of Process Engineering, University of Constantine 3, 25000 Constantine, Algeria

* E-mail: kerabchi_nassim@yahoo.fr

Abstract

The chemical effects of ultrasound (sonochemistry) originate from acoustic cavitations, that is, ultrasound-induced formation, growth and violent collapse of micro bubbles in a liquid medium. The rapid collapse of cavitation bubbles is nearly adiabatic, rendering each individual bubble a microreactor, inside which temperatures of the order of 5000 K and pressures of hundreds of atmospheres have been shown to exist. This work presents results of a comprehensive numerical assessment of chemical reactions occurring in an O_2-bubble oscillating in water irradiated by an ultrasonic wave. Simulations have been performed for diverse combinations of various parameters such as ultrasound frequency (20–1000 kHz),static pressure (0.5–2 atm) and liquid temperature (20–50 °C). The aim of this series of computations was to correlate the production of $HO^{\bullet}$ and hydrogen to the temperature and pressure achieved in the bubble during the strong collapse. The obtained results clearly showed the existence of an optimum bubble temperature of about 4200 °C and pressure of about 2000 atm. The predicted value of the bubble temperature for the production of $HO^{\bullet}$ and hydrogen is in excellent agreement with that determined experimentally. The existence of an optimum bubble temperature and pressure in collapsing bubbles results from the competition between reactions of production and those of consumption of $HO^{\bullet}$ radicals at very high temperatures.

***Keywords**: Sonochemistry, Acoustic cavitation, Hydroxyl radical ($HO^{\bullet}$)*

I. Introduction:

When an ultrasonic wave propagates through a liquid, the local pressure varies with time and space. If a bubble is present in the liquid, its radius will expand and con-tract in response to these pressure changes. For low amplitude pressure excursions, these oscillations are sinusoidal and may last for many acoustic cycles, a phenomenon called stable cavitation. Under certain conditions, however, these oscillations may become unstable leading to the rapid collapse of a bubble during a single acoustic half-cycle. This phenomenon is called transient cavitation. High temperatures and pressures are generated within the bubble during its final stage of collapse that is thought to produce hydrogen atoms and hydroxyl radicals in aqueous solutions. Some investigators feel that temperatures sufficient to generate free radicals are sometimes produced for stable cavitations as well [1]. In the present study, we have theoretically estimated the optimum temperature of collapsing bubble for the production of HO● and hydrogen. The used model combines the dynamic of bubble collapse in acoustical field propagated in water with a chemical kinetics consisting in nineteen reversible chemical reactions occurring thigh temperatures during the strong collapse of the bubble. A series of computations were performed for more than 300 combinations between various parameters including ultrasound frequency in the range 20–1000 kHz, static pressure (0.5–2 atm) and liquid temperature (20–50 °C).

II.Model and computational methods:

II.1 Bubble dynamics model

The theoretical model used in the present computational study have been fully described in refs. [2, 3]. It combines the dynamic of single bubble in acoustic field with chemical kinetics consisting of a series of chemical reactions occurring in the bubble at the collapse phase. The following is a brief description of the model. A gas and vapor filled spherical bubble isolated in wateroscillates under the action of a sinusoidal sound wave. The temperature and pressure in the bubble are assumed spatiallyuniform and the gas content of the bubble behaves as an ideal gas [4].The radial dynamics of the bubble is described by theKeller-Miksisequation that includes first order terms in the Mach number M ¼ Ṙ/c [5, 6]:

$$\left(1-\frac{\dot{R}}{c}\right)R\ddot{R}+\frac{3}{2}\left(1-\frac{\dot{R}}{3c}\right)\dot{R}^{2}=\frac{1}{\rho_{L}}\left(1+\frac{\dot{R}}{c}+\frac{R}{c}\frac{d}{dt}\right)\left[p_{B}-P(t)\right] \quad (1)$$

$$P_{B}=p-\frac{2\sigma}{R}-4\mu\frac{\dot{R}}{R} \quad (2)$$

$$P(t)=P_{\infty}-P_{A}\sin(2\pi ft) \quad (3)$$

II.2 Chemical kinetics model :

A kinetics mechanism consisting in 25 chemical reactions and their backwards reactions (Table 1) is taken into account involving AR, O2, H2O, OH, H, O, HO2, H2 and H2O2 species. The scheme in Table 1 has been partially validated from hydrogen flame studies [7] as well as shock-tube and reactor-type experiments [8].

Rate expressions for the chemical reactions consider elementary reversible reactions involving K chemical species, which can be represented in the general form as

$$\sum_{k=1}^{K}\upsilon'_{ki}X_{k}\leftrightarrow\sum_{k=1}^{K}\upsilon''_{ki}X_{k}\quad(i=1,\ldots,I)$$

in which ϑ_{ki} is the stoichiometric coefficients of the itch reaction and X_k is the chemical symbol for the kth species. The superscript ‘ indicates forward stoichiometric coefficients, while “ indicates reverse stoichiometric coefficients. The production rate of the kth species can be written as asummation of the rate of the variables for all reactions involving the kth species:

$$\dot{w}_k = \frac{d[X_K]}{dt} = \sum_{i=1}^{I} (\upsilon''_{ki} - \upsilon'_{ki}) r_i \qquad (k= 1.....K) \tag{4}$$

The rate r_i for the ith reaction is given by the difference of the forward and reverse rates as

$$r_i = k_{f\,i} \prod_{k=1}^{K} [X_k]^{\upsilon'_{ki}} - k_{r\,i} \prod_{k=1}^{K} [X_k]^{\upsilon''_{ki}} \tag{5}$$

Where $[X_k]$ is the molar concentration of the kth species and k_{fi} andk_{ri} are the forward and reverse rate constants of the ith reaction, respectively. The forward and reverse rate constants for the ithreactions are assumed to have the following Arrhenius temperature dependence:

Table 1 :Scheme of the possible chemical reactions inside a collapsing O_2 bubble [9,10,11,12,13,14]. M is the third body. Subscript "f" denotes the forward reaction and "r" denotes the reverse reaction. A is in ($cm^3mol^{-1}s^1$) for two body reaction [($cm^6mol^{-2}s^{-1}$) for a three body reaction], and Ea is in (cal mol^{-1}).

N°	Réaction	A_f	b_f	E_{af}	A_r	b_r	E_{ar}
1.	$H_2O+M \leftrightarrow H^{\bullet}+{}^{\bullet}OH+M$	1.912×10^{23}	-1.83	1.185×10^{5}	2.2×10^{22}	-2.0	0.0
2.	$O_2+M \leftrightarrow O+O+M$	4.515×10^{17}	-0.64	1.189×10^{5}	6.165×10^{15}	-0.5	0.0
3.	${}^{\bullet}OH+M \leftrightarrow O+H^{\bullet}+M$	9.88×10^{17}	-0.74	1.021×10^{5}	4.714×10^{18}	-1.0	0.0
4.	$H^{\bullet}+O_2 \leftrightarrow O+{}^{\bullet}OH$	1.915×10^{14}	0.0	1.644×10^{4}	5.481×10^{11}	0.39	-2.93×10^{2}
5.	$H^{\bullet}+O_2+M \leftrightarrow HO_2^{\bullet}+M$	1.475×10^{12}	0.6	0.0	3.09×10^{12}	0.53	4.887×10^{4}
6.	$O+H_2O \leftrightarrow {}^{\bullet}OH+{}^{\bullet}OH$	2.97×10^{6}	2.02	1.34×10^{4}	1.465×10^{5}	2.11	-2.904×10^{3}
7.	$HO_2^{\bullet}+H^{\bullet} \leftrightarrow H_2+O_2$	1.66×10^{13}	0.0	8.23×10^{2}	3.164×10^{12}	0.35	5.551×10^{4}
8.	$HO_2^{\bullet}+H^{\bullet} \leftrightarrow {}^{\bullet}OH+{}^{\bullet}OH$	7.079×10^{13}	0.0	2.95×10^{2}	2.027×10^{10}	0.72	3.684×10^{4}
9.	$HO_2^{\bullet}+O \leftrightarrow {}^{\bullet}OH+O_2$	3.25×10^{13}	0.0	0.0	3.252×10^{12}	0.33	5.328×10^{4}
10.	$HO_2^{\bullet}+{}^{\bullet}OH \leftrightarrow H_2O+O_2$	2.89×10^{13}	0.0	-4.97×10^{2}	5.861×10^{13}	0.24	6.908×10^{4}
11.	$H_2+M \leftrightarrow H^{\bullet}+H^{\bullet}+M$	4.577×10^{19}	-1.4	1.044×10^{5}	1.146×10^{20}	-1.68	8.2×10^{2}
12.	$O+H_2 \leftrightarrow H^{\bullet}+{}^{\bullet}OH$	3.82×10^{12}	0.0	7.948×10^{3}	2.667×10^{4}	2.65	4.88×10^{3}
13.	${}^{\bullet}OH+H_2 \leftrightarrow H^{\bullet}+H_2O$	2.16×10^{8}	1.52	3.45×10^{3}	2.298×10^{9}	1.40	1.832×10^{4}
14.	$H_2O_2+O_2 \leftrightarrow HO_2^{\bullet}+HO_2^{\bullet}$	4.634×10^{16}	-0.35	5.067×10^{4}	4.2×10^{14}	0.0	1.198×10^{4}
15.	$H_2O_2+M \leftrightarrow {}^{\bullet}OH+{}^{\bullet}OH+M$	2.951×10^{14}	0.0	4.843×10^{4}	1.0×10^{14}	-0.37	0.0
16.	$H_2O_2+H^{\bullet} \leftrightarrow H_2O+{}^{\bullet}OH$	2.410×10^{13}	0.0	3.97×10^{3}	1.269×10^{8}	1.31	7.141×10^{4}
17.	$H_2O_2+H^{\bullet} \leftrightarrow H_2+HO_2^{\bullet}$	6.025×10^{13}	0.0	7.95×10^{3}	1.041×10^{11}	0.70	2.395×10^{4}
18.	$H_2O_2+O \leftrightarrow {}^{\bullet}OH+HO_2^{\bullet}$	9.550×10^{6}	2.0	3.97×10^{3}	8.66×10^{3}	2.68	1.856×10^{4}
19.	$H_2O_2+{}^{\bullet}OH \leftrightarrow H_2O+HO_2^{\bullet}$	1.0×10^{12}	0.0	0.0	1.838×10^{10}	0.59	3.089×10^{4}
20.	$O_2+O+M \leftrightarrow O_3+M$	4.1×10^{12}	0.0	-2.114×10^{3}	2.48×10^{14}	0.0	2.286×10^{4}
21.	$OH+O_2+M \leftrightarrow +O_3+H$	4.4×10^{7}	1.44	7.72×10^{4}	2.3×10^{11}	0.75	0.0
22.	$O_3+H \leftrightarrow HO_2+O$	4.1×10^{12}	0.0	-2.114×10^{3}	-	-	-
23.	$O_3+O \leftrightarrow O_2+O_2$	5.2×10^{12}	0.0	4.18×10^{3}	-	-	-
24.	$O_3+OH \leftrightarrow O_2+HO_2$	7.8×10^{7}	0.0	1.92×10^{3}	-	-	-
25.	$O_3+HO_2 \leftrightarrow O_2+O_2+OH$	1.0×10^{11}	0.0	2.82×10^{3}	-	-	-

$$k_{f\,i} = A_{f\,i} T^{b_{f\,i}} \exp\left(-\frac{E_{a\,f\,i}}{R_g T}\right) \quad (6)$$

$$k_{r\,i} = A_{r\,i} T^{b_{r\,i}} \exp\left(-\frac{E_{a\,r\,i}}{R_g T}\right) \quad (7)$$

where R_g is the universal gas constant, A_{fi} (A_{ri}) is the preexponential factor, b_{fi} (b_{ri}) is the temperature exponent and E_{fi} (E_{ri}) is the activation energy. Arrhenius parameters of each chemical reaction are listed in Table 1.In some reactions of Table 1, a third body is required for the reaction to process. When a third body is needed, the

reaction rate ri of the ith reaction should be rewritten as

Procedure of the numerical simulation:

The KellerMiksis equation (Eq. (1)), describing the dynamic of the bubble, is a non-linear second-order differential equation which requires an approximate numerical method for solution Eq. (1) can be reduced to a system of two differential first order equations

$$\frac{dR}{dt} = \dot{R} \quad (8)$$

$$\frac{d\dot{R}}{dt} = \ddot{R} = \frac{\frac{1}{\rho_L}\left(1+\frac{\dot{R}}{c}+\frac{R}{c}\frac{d}{dt}\right)[p_B - P(t)] - \frac{3}{2}\left(1-\frac{\dot{R}}{3c}\right)\dot{R}^2}{\left(1-\frac{\dot{R}}{c}\right)R} \quad (9)$$

The system of Eqs. (8) and (9) was solved by the fourth order Runge_Kutta method using the following initial conditions:

T= 0; R=R0 and _R = 0

The physical properties used for numerical calculations are given for water at 20 °C as .ρ_L =998.12 kg m^{-3}, s=72.45* 10^{-3}Nm^{-1}, μ= 10^{-3} kg $s^{-1}m^{-1}$ and c= 1482ms^{-1}.

The simulation of the chemical reactions in the bubble starts at the beginning of the adiabatic phase (at time corresponding to R =Rmax). The application of Eq. (4) for all species (9 species) involved in the scheme of Table 1 gives a system of nine ordinary differential equations. For example, according to Table 1, the application of Eq. (4) to the H2O species gives:

$$\begin{aligned} w_k = \frac{1}{V}\frac{dn_{H_2O}}{dt} = &-\left\{k_{f1}[H_2O][M] - k_{r1}[H^\bullet][^\bullet OH][M]\right\} - \left\{k_{f6}[H_2O][O] - k_{r6}[^\bullet OH]^2\right\} - \\ &\left\{k_{f10}[HO_2^\bullet][^\bullet OH] - k_{r10}H_2O][O_2]\right\} - \left\{k_{f13}[H_2][^\bullet OH] - k_{r13}[H_2O][H]\right\} - \\ &\left\{k_{f16}[H_2O_2][H^\bullet] - k_{r16}[H_2O][^\bullet OH]\right\} - \left\{k_{f19}[H_2O_2][^\bullet OH] - k_{r19}[H_2O][HO_2^\bullet]\right\} \end{aligned} \quad (10)$$

When V is the volume of the bubble and nH2O is the number of moles of H2O. Using the ideal-gas law PV = n_tRT, Eq. (10) can be rewritten:

$$\frac{dn_{H_2O}}{dt} = -\frac{n_t RT}{p}\left\langle \begin{array}{l} \{k_{f1}[H_2O][M] - k_{r1}[H^\bullet][^\bullet OH][M]\} - \{k_{f6}[H_2O][O] - k_{r6}[^\bullet OH]^2\} - \\ \{k_{f10}[HO_2^\bullet][^\bullet OH] - k_{r10}H_2O][O_2]\} - \{k_{f13}[H_2][^\bullet OH] - k_{r13}[H_2O][H]\} - \\ \{k_{f16}[H_2O_2][H^\bullet] - k_{r16}[H_2O][^\bullet OH]\} - \{k_{f19}[H_2O_2][^\bullet OH] - k_{r19}[H_2O][HO_2^\bullet]\} \end{array} \right\rangle \quad (11)$$

where n_t is number of mole of all species present in the bubble. The input parameters for solving the system of the ordinary differential equations obtained by Eq. (4) are the composition of the bubble on water vapor and argon at time corresponding to R = Rmax, the temperature and pressure profiles in the bubble during adiabatic phase and the collapse time. These parameters are obtained by solving the dynamic Equation (Eq. (1)). As the bubble temperature increases during the adiabatic phase, the reaction system evolves and radicalsstart to form by thermal dissociation of H2O in the bubble.Thus, the composition of the bubble on all species expected tobe present was determined at any temperature during thecollapse period by solving the system of the ordinary differentialequations obtained by Eq. (4). The system of the ordinarydifferential equations was solved by the finite differencemethod. The computer simulation of the reactions systemwas stopped after the end of the bubble collapse.

III. Results and discussion:

The maximum bubble temperature and pressure attained in the interior of the acoustic bubble is another characteristic of acoustic bubbles. There have been several methods reported to date for determining bubble temperatures in water [15, 16] and in other fluids [17]. Experimental estimation of the temperature within the collapsing bubbles based on multibubble sonochemistry and emissions from excited species (sonoluminescence) are reported to be between 750 K and 6000 K [18]. The reason for this range is in part due to the different methods employed to determine the temperature and in part due to the different experimental conditions/systems used. Using the model described in section 2, we have estimated the optimum bubble temperature and pressure reached in the bubble using the production of •OH and hydrogen. A series of computations of the bubble oscillation and the chemical reactions occurring inside a bubble at the collapse were conducted for various experimental parameters including ultrasonic frequency (20–1000 kHz), static pressure (0.5–2 atm) and liquid temperature (20–50 °C). For more than 300 points of combination between these different operating parameters, the mole fraction of •OH radical and hydrogen created

in the bubble per collapse for each case of the diverse combinations was related to the corresponding maximum temperature and pressure achieved in the bubble at the collapse. The correlation between the bubble temperature and the mole fraction of •OH radicals and hydrogen created per collapse is shown in Figure 1a and Figure 2a [19]. The correlation between the pressure inside a bubble at the collapse and the mole fraction of •OH radicals formed and hydrogen in the bubble per collapse is shown in Figure 1b and Figure 2b. From these figures, it is clearly showed that there exist optimum bubble temperatures of

about 4000 K and pressure of about 1500 atm for the production of •OH radicals, and 4000 K and pressure of about 1000 atm for the production of hydrogen. Suslick and coworkers estimated, by kinetic measurements, a maximum bubble temperature of 5200 ± 650 K [8]. They also determined a temperature of 5100 ± 200 K, using spectroscopic measurements during multibubble sonoluminescence emitted from excited states of free metal atoms [15]. the optimum bubble temperature predicted in our study (5200 K) is in excellent agreement with the experimentally estimated bubble temperatures. Additionally. Upon stronger acoustic driving of the bubble, they estimated a maximum pressure of about 3700 atm [20]. Thus, the optimum value of pressure, 2500 atm, predicted in our theoretical study for oxygen bubble is in the same order of magnitude with the experimentally estimated pressures.

Several reactions are responsible for the production of •OH inside a bubble and several other reactions are responsible for their consumption. Yasui et al. [21], using a more detailed model, predicted an optimum bubble temperature of about 5500 K for the production of the oxidants in an air bubble when the ultrasonic frequency is 140 kHz. This result was justified [50] by the strong consumption of the oxidant by the oxidizing nitrogen at higher bubble temperatures (>5500 K). In our cases (O2 bubble), the existence of an optimum

radicals may be attributed to the competition between the reactions of production and those of consumption of •OH radicals at high temperatures. Based on the results of Figures 6a and 6b, it can be seen that for temperatures and pressures less than 4000 K and 1500 atm respectively, linear evolutions of the valleys of points constituting the mole fractions of •OH radicals created per collapse as function of temperature (Figure 1a) and pressure (Figure 2b) are observed. So, we can make a decision that the reactions of consumption have no significant impact when the bubble temperature and pressure are less than 4000 K and 1500 atm, respectively and, thus, the reactions of production are always dominant. However, when the bubble temperature and pressure exceed 4000 K and 1500 atm respectively, we observe a decline in the valleys of Figures 1a and Figures 1b indicating that the reactions of consumption are started to take place by scavenging •OH radicals. The scavenging effect of the consumption reactions continues to increase with the internal temperature and pressure above 4000 K and 1500 atm to finally yield an optimum temperature of around 4000 K and pressure of around 1500 atm for the production of •OH radicals. This is possibly the unique reason for the existence of an optimum bubble temperature and pressure for the production of the •OH radicals and hydrogen, in the collapsing bubbles.

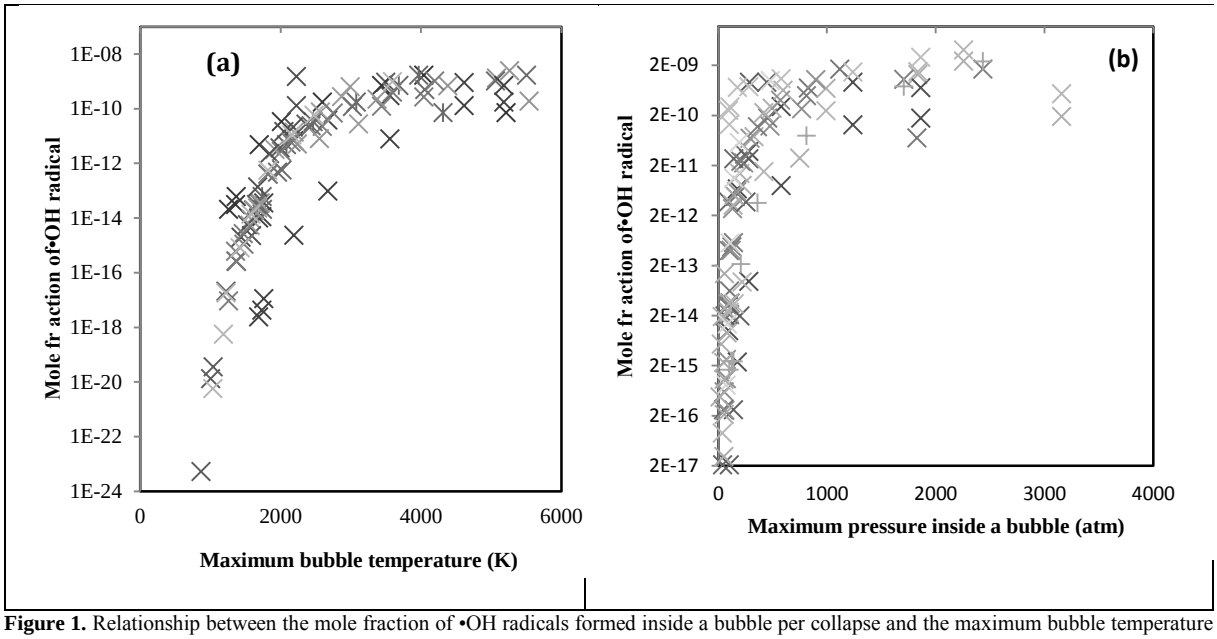

Figure 1. Relationship between the mole fraction of •OH radicals formed inside a bubble per collapse and the maximum bubble temperature (a) and pressure (b) achieved at the collapse.

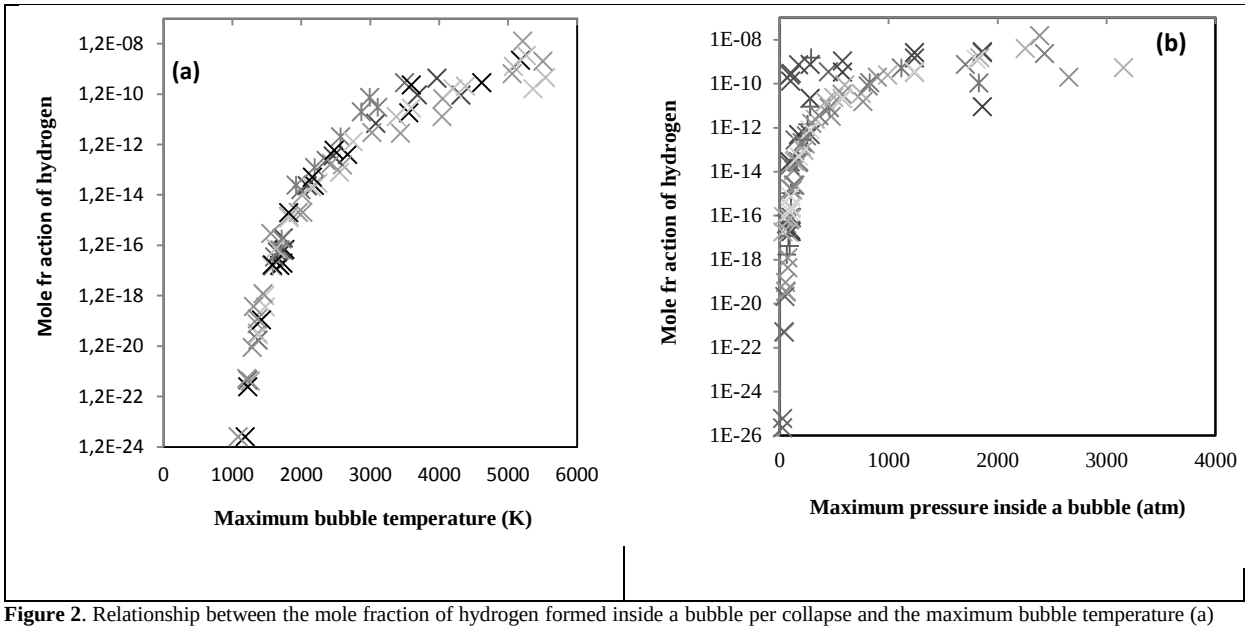

Figure 2. Relationship between the mole fraction of hydrogen formed inside a bubble per collapse and the maximum bubble temperature (a) and pressure (b) achieved at the collapse.

IV. Conclusion

In this study, we performed a series of simulations of chemical reactions inside an isolated spherical bubble oscillating in water irradiated by an ultrasonic wave. The simulations were performed for diverse combinations (more than 300 points) of various parameters such as ultrasound frequency (20–1000 kHz)static pressure (0.5–2 atm) and liquid temperature (20–50 °C). The aim of this series of computations was to correlate the production of HO● and hydrogen to the temperature and pressure achieved in the bubble during the strong collapse. The obtained results clearly showed the existence of an optimum bubble temperature of about 4000 °C and pressure of about 2000 atm. The predicted value of the bubble temperature for the production of HO● and hydrogen is in excellent agreement with that determined experimentally. The existence of an optimum bubble temperature and pressure in collapsing bubbles results from the competition between reactions of production and those of consumption of HO● radicals at very high temperatures.

V. References

[1] P. Riesz, D. Berdahl and C. L. Christman. Free Radical Generation by Ultrasound in Aqueous and Nonaqueous Solutions.Environmental Health **Perspectives Vol. 64, pp. 233-252, 1985**

[2] Merouani S, Hamdaoui O, Rezgui Y, Guemini M. Mechanism of sonochemical

production of hydrogen. Int J Hydrogen Energy 2015;40:4056e64.

[3] Merouani S, Hamdaoui O, Rezgui Y, Guemini M. Theoretical procedure for the characterization of acoustic cavitation bubbles. ActaAcust United Acust 2014;100:823e33.

[4] Merouani S, Hamdaoui O, Rezgui Y, Guemini M. Theoretical estimation of the temperature and pressure within collapsing acoustical bubbles. UltrasonSonochem

2014;21:53e9.

[5] Crum LA. The polytrophic exponent of gas contained within air bubbles pulsating in a liquid. J AcoustSoc Am 1983;73:116e20.

[6] Keller JB, Kolodner II. Damping of underwater explosion bubble oscillations. J ApplPhys 1956;27:1152e61.

[7] Burdin F, Tsochatzidis NA, Guiraud P, Wilhelm AM, Delmas H. Characterisation of the acoustic cavitation

cloud by two laser techniques. UltrasonSonochem 1999;6:43e51.

[8] Ohl C, Kurz T, Geisler R, Lindau O, Lauterborn W. Bubbledynamics, shock waves and

sonoluminescence. Philos Trans R SocLond A 1999;357:269e94.

[9] Hart EJ, Henglein A. Sonochemistry of aqueous solutions: H2eO2 combustion in cavitation bubbles. J PhysChem1987;91:3654e6.

[10] Adewuyi YG. Sonochemistry: environmental science and engineering applications. IndEngChem Res

2001;40:4681e715.

[11] Merouani S, Hamdaoui O, Rezgui Y, Guemini M. A method for predicting the number of active bubbles in sonochemicalreactors.UltrasonSonochem 2015;22:51e8.

[12] Crum LA. The polytrophic exponent of gas contained within air bubbles pulsating in a liquid. J AcoustSoc Am 1983;73:116e20.

[13] Keller JB, Miksis MJ. Bubble oscillations of large amplitude. J AcoustSoc Am 1980;68:628e33.

[14] Colussi AJ, Weavers LK, Hoffmann MR. Chemical bubble dynamics and quantitative sonochemistry. J PhysChem A 1998;102:6927e34.

[15] K. S. Suslick, D. J. Flannigan: Inside a collapsing bubble: Sonoluminescence and the conditions during cavitation. Annu. Rev. Phys. Chem. 59 (2008) 659–683.

[16] K. S. Suslick, D. A. Hammerton, R. E. J. Cline: Sonochemical hotspot. J. Am. Chem. Soc. 108 (1986) 5641–5642.

[17] P. M. Kanthale, M. Ashokkumar, F. Grieser: Estimation of cavitation bubble temperatures in an ionic liquid. J. Phys. Chem. C 111 (2007) 18461–18463.

[18] K. S. Suslick: Ultrasound: its chemical, physical and biological effects. VCH Publishers, New York, 1988.

[19] S. Merouani, O. Hamdaoui, Y. Rezgui, M. Guemini: Theoretical estimation of the temperature and pressure within collapsing acoustical bubbles. Ultrason. Sonochem. 21 (2014) 53–59.

[20] D. J. Flannigan, S. D. Hopkins, C. G. Camara, S. J. Putterman, K. S. Suslick: Measurement of pressure and density inside a single sonoluminescing bubble. Phys. Rev. Lett. 96 (2006) 204301–1 – 204301–4.

[21] K. Yasui, T. Tuziuti, Y. Iida: Optimum bubble temperature for the sonochemical production of oxidants. Ultrasonics (2004) 579–584.

Nomenclature

c: Speed of sound in the liquid medium, m s^1

f: Frequency of ultrasonic wave, Hz

I: Acoustic intensity of ultrasonic irradiation, W m^{-2}

p: Pressure inside a bubble, Pa

p_{max}: Maximum pressure inside a bubble, Pa

p_{∞}: Ambient static pressure, Pa

P_A: Amplitude of the acoustic pressure, Pa

Pv: Vapor pressure of water, Pa

Pg0: Initial gas pressure, Pa

R: Radius of the bubble, m

Rmax: Maximum radius of the bubble, µm

R0: Ambient bubble radius, µm

t: Time, s

T: Temperature inside a bubble, K

Tmax: Maximum temperature inside a bubble, K

T_{∞}: Bulkliquidtemperature, K

σ: Surface tension of liquid water, N m^{-1}

ρ: Density of liquid water, kg m^{-3}